Computational Fluid Dynamics Analysis of 3D Wind Flow around Rhizophora Mangrove Tree and Drag Force Acting on the Wall of the Tree

SINI RAHUMAN[1], MOHAMED ISMAIL[2], SHYLA MANAVALAN VARGHESE[3], BINSON V. A.[4]
[1]Faculty of Foundation (Mathematics),
Bahrain Polytechnic,
Isa Town,
KINGDOM OF BAHRAIN

[2]Department of Mathematics,
Sathyabama Institute of Science and Technology,
Chennai,
INDIA

[3]Department of Developmental Mathematics,
Houston Community College,
Houston, Texas,
USA

[4]Department of Electronics Engineering,
Saintgits College of Engineering,
INDIA

Abstract: - Many natural disasters, such as cyclones, typhoons, mudslides, and tsunamis, are currently plaguing the world. These tragedies, which have destroyed the coastal settlements, claim a great number of lives each year. The characteristics and structure of the Mangrove tree have the significant impact on protecting the coast from heavy wind, floods, mudslides, and other kinds of natural disasters. This research work investigates how Mangroves can protect the area near the coast from a fluid dynamics point of view. Complex real world problems require intelligent systems that combine knowledge and techniques. Hence Computational Fluid Dynamics (CFD) technique namely the finite volume method is employed as a tool in this study. In this research, a model Rhizophora Mangrove tree from Pichavaram Mangrove forest, Tamilnadu, India is generated using Ansys Workbench design modeler. A computational domain is created around this tree to reduce the boundary effect. Grid-independent research was carried out using various mesh sizes to determine the best grid resolution for the analysis. An unstructured triangular mesh was generated for the simulation. The focus of this study is to determine the 3D flow around the tree in order to determine the wind velocity, as well as the coefficient of drag and drag force on the wall tree. This research helps to give a clear understanding of wind flow around the 3D Rhizophora Mangrove tree. The velocity profile, pressure distribution, drag force, and drag coefficient around the tree are captured, analysed, and presented in detail. The results show that the Rhizophora mangrove trees can significantly reduce the flow velocity of the wind and will be able to safeguard the coast and communities nearby from natural disasters.

Key-Words: - Rhizophora, wind velocity, steady flow, unsteady flow, coefficient of drag force, computational fluid dynamics.

Received: January 17, 2023. Revised: November 22, 2023. Accepted: December 19, 2023. Published: December 31, 2023.

1 Introduction

Natural disasters are a huge danger to human beings all around the earth every year. To defend the coastline from tsunamis, storms, floods, tornadoes, and hurricanes, coastal erosion is a serious challenge. A mangrove is a shrub or tree that lives in salty or brackish water along the coast. They shield the surrounding areas from tsunamis and poor

weather. Planting mangroves near the coast is one of the most effective ways to defend the coast, as mangroves can break up fluid movement. In 2004, the Indian Ocean Tsunami caused damage to a number of Asian and African countries. Many villages located behind the forest were sheltered by the mangrove forest during the Tsunami, according to studies, [1].

Various numerical and analytical research, [2], [3], [4], [5], [6], [7], [8], [9], [10], [11], [12], [13], [14], [15], [16], [17], [18] have been undertaken to examine and discover the importance of mangrove forests. To examine wave attenuation over a finite-area vegetated region, researchers, [19], established a computer model based on small-amplitude periodic waves traveling through a lattice-like structure of vertical cylinders. Researchers developed a refraction-diffraction wave model, [20], for analyzing wave propagation along a moderate slope zone on the shore in the presence of stiff vegetation. A 3-D numerical technique was used to explore the interaction of tsunami waves with mangrove ecosystems, [21]. In a recent work [22], numerical analysis was utilized to investigate periodic long-wave run-ups on sloping beaches with stiff vegetation. Another study [23], used a 2-D Numerical Wave Tank based on a porous body model to show energy dissipation after contact with a tsunami. The results reveal that when plant height, density and width increase, the coefficient of transmission decreases but the reflection coefficient remains constant.

Another study [24], revealed that in regions with extensive mangrove trees, waves traveling through the roots generate jets, which like to move around and cause turbulence. According to the study, friction between the mangrove forest and the waves slows the velocity of the waves, as contrasted to friction at the bottom. The wave height and drop in water velocity differ depending on the type of mangrove species, [25]. Some researchers, [26], used a computer simulation to explore the features of roots and their involvement in reducing the velocity of water flow around Avicennia marina and Rhizophora apiculate.

In [27], a three-dimensional numerical technique based on IHFOAM was used to explore the interaction of tsunami waves with mangrove forests. Research carried out using green infrastructure and coastal ecosystems offers a natural approach method to overcome natural disasters, [28]. Another study was conducted and included a detailed explanation regarding the supplementary proof of the storm protection ecosystem services offered by mangroves in the area. This serves as an additional justification for investing in mangrove ecosystems to enhance resilience against coastal disasters such as storms, [29]

The velocity of waves was reduced as the breadth and density of the forest grew, according to data acquired from Avicennia's numerical simulation with the TUNA-RP model, [30]. According to a numerical simulation study, [31], on energy dissipation within the mangrove forest, the mean wave velocity decreased considerably for every 20 m cross-section of the mangrove forest. The flow's vertical and horizontal amplitude velocities were both reduced by around 60% of their original velocity, [32].

According to a CFD study, [3], mangrove roots have an important role in lowering wave velocity and protecting the coast. CFD has also been used to study the vortex activity related to gravitational water vortex power plants, [33].CFD investigation of water flow patterns around the rhizophora tree was conducted in [5] and it was revealed that the fluid velocity was lowered by more than 70%.The behavior and efficacy of stilt roots (prop roots) of Rhizophora Mangroves in lowering the flow of the velocity of the wind during severe tropical storms, intense tropical cyclones, and extremely intense tropical cyclones were analyzed in [34].

The goal of this study is to identify the 3D wind flow around the Rhizophora mangrove tree using a computational approach to analyze and discover the efficiency of mangroves in reducing flow velocity. To develop shoreline protection systems and promote the planting of mangrove trees around the coast to safeguard villages near the coast, it is critical to strengthen and expand research in wave velocity propagation across Mangrove forests in actual weather scenarios.

2 Methodology

2.1 Study Approach

Pichavaram Mangrove Forest stands as India's renowned and the world's second-largest mangrove expanse. The M.S. Swaminathan Research Foundation (MSSRF) in Chennai has meticulously gathered data on the Rhizophora Mangrove tree indigenous to Pichavaram. This valuable dataset serves as the foundation for creating a computational model of the Rhizophora Mangrove tree. Such modeling aids in a deeper understanding of the tree's ecological dynamics, supporting conservation initiatives and promoting sustainable

management practices in the Pichavaram Mangrove forest.

This study (CFD) starts with the development of a computational model of the Rhizophora mangrove tree, which is visualized in Figure 1. Ansys Workbench design modeler 18.1 is used for this process in general. The mesh is generated around this geometry and applied to the boundary condition. Fine mesh is generated near and around the roots as visualized in Figure 2. Iso surface created at y=0.25m, z=0.25m, y=0.75m &z=0.75m, which are shown in Figure 3 and Figure 4. The problem is solved using Ansys fluent CFD software. The CFD, k- epsilon turbulence model is used to simulate the incompressible steady and unsteady wind flow around the Rhizophora mangrove tree.

The following two cases are analyzed in this study and this problem is solved using the finite volume method.

Case 1: Steady incompressible turbulent flow with velocity 50m/s

Case2: Unsteady incompressible turbulent flow with velocity 50m/s

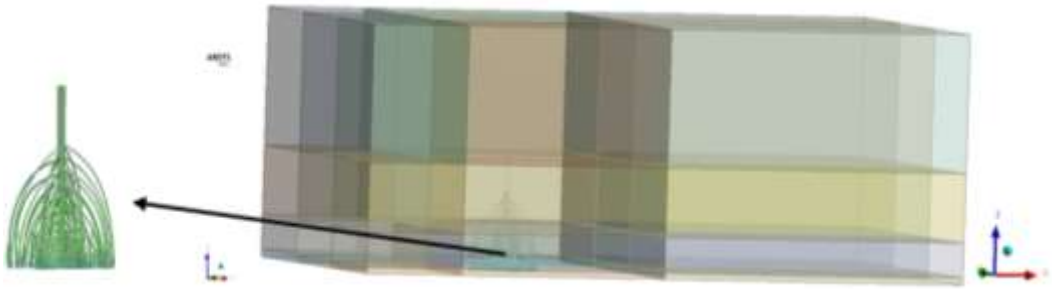

Fig. 1: Geometry created in Ansys workbench 18.1

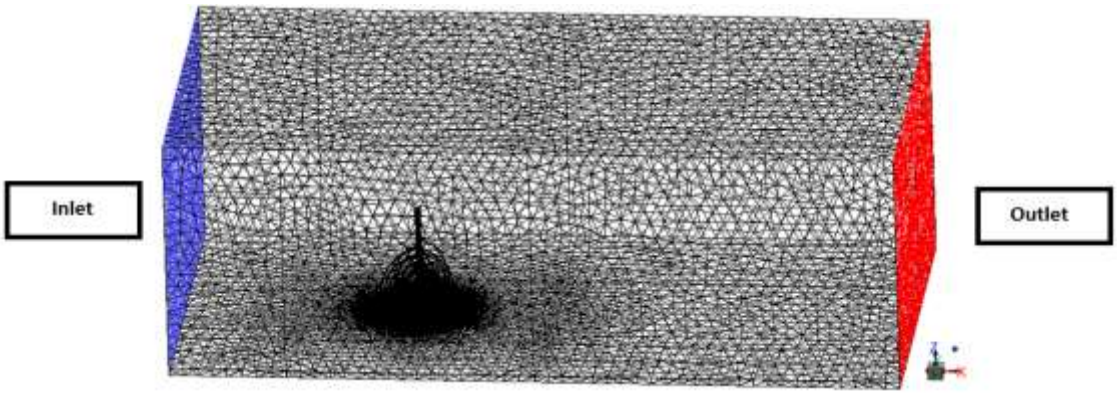

Fig. 2: Mesh created in Ansys design modeler

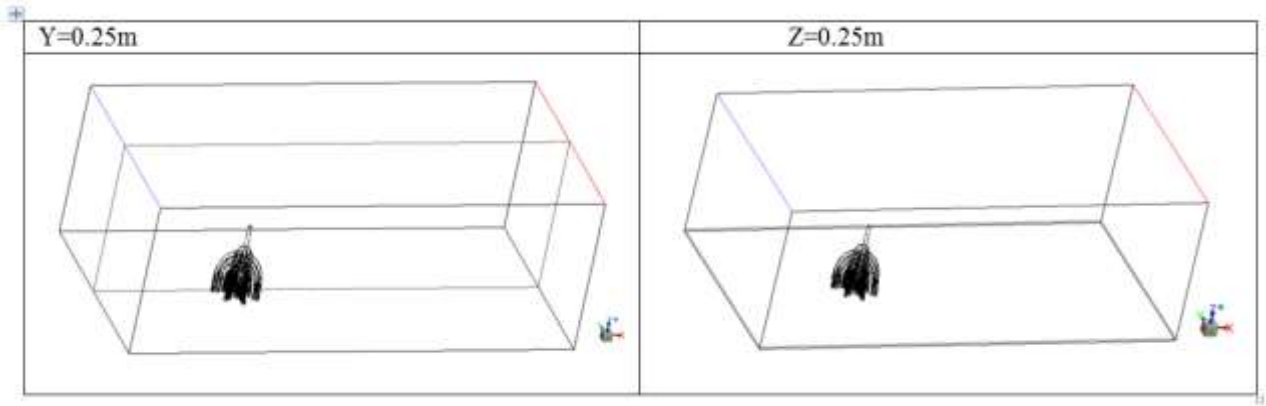

Fig. 3: Iso surface created at Y=0.25m & Z=0.25m

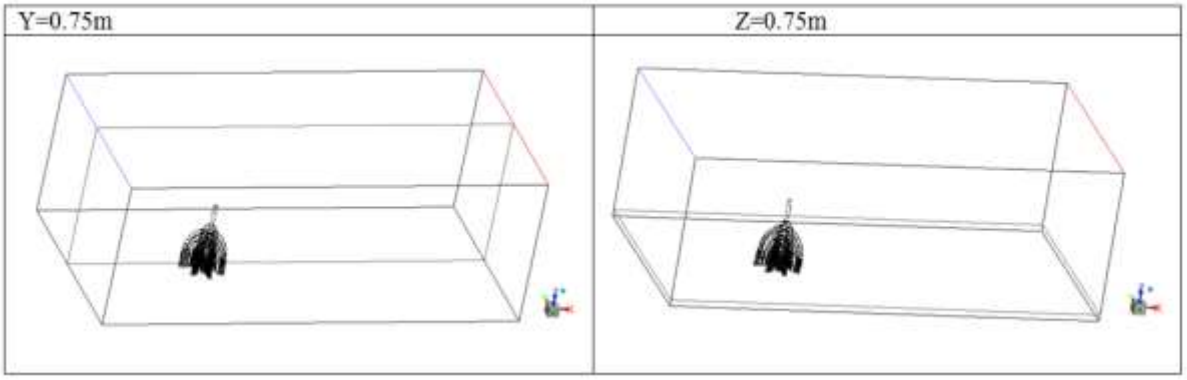

Fig. 4: Iso surface created at Y=0.75m & Z=0.75m

2.2 Governing Differential Equation

1)Navier-Stokes system of equations for a three-dimensional, incompressible flow,

Continuity Equation: $\frac{\partial \rho}{\partial t} + \nabla.(\rho \vec{q}) = 0$ (1)

x-momentum equation:

$\left(\frac{\partial(\rho u)}{\partial t} + \nabla.(\rho u \vec{q})\right) = -\frac{\partial p}{\partial x} + \nabla.(\mu \nabla u)$ (2)

y-momentum equation:

$\left(\frac{\partial(\rho v)}{\partial t} + \nabla.(\rho v \vec{q})\right) = -\frac{\partial p}{\partial y} + \nabla.(\mu \nabla \mathrm{v})$ (3)

z-momentum

$\left(\frac{\partial(\rho w)}{\partial t} + \nabla.(\rho w \vec{q})\right) = -\frac{\partial p}{\partial z} + \nabla.(\mu \nabla \mathrm{w})$ (4)

Were the velocity vector ,$\vec{q} = u\vec{\imath} + v\vec{j} + w\vec{k}$ with *u*, *v*, and *w* representing the velocity components in the x, y, and z directions.μ is coefficient of viscosity, ρ is density, p is pressure and t is time. For steady state conditions, the rate of change term, which is the first term on the left hand side in the equations, equals zero.

2) Drag Force

$F = ½\ \rho\ V^2 A\ C_D$ (5)

F is drag force (kN);V is velocity (m/s);C_D is Drag Coefficient and A is Frontal Area(m^2) andρ is air density (Kg/m^3).

2.3 Boundary Condition

This study is conducted by Computational fluid dynamics using ansys software and the boundary conditions were implemented on the mesh model. The steady and unsteady three-dimensional airflow simulation was driven by the inlet velocity of 50m/s.At the outlet, zero-gauge pressure was applied. In this study, the Reynolds number is more than 500000, and the k-epsilon turbulence model is applied to simulate the flow. All body forces are ignored and the walls are stationary (no slip boundary condition). No slip boundary condition is applied to the wall and all body forces are neglected.

This flow has a mach number of less than 0.3, indicating that it is an incompressible viscous flow. The density of air is 1.225 kg/m3 in this research, and the coefficient of viscosity of the air is 1.7894e-05 kg/m-s in Cases 1 and 2.

2.4 Grid Independent Study

Ansys workbench design Modeler is used to create a 3D model of the Rhizophora Mangrove tree, and Ansys fluent is used to simulate steady and unsteady velocity and also identify the coefficient of drag and drag force on the wall tree. Tetrahedral grids are used for meshing the surface of the mangrove tree model in this work after comprehensive verification. Finer grids were chosen along the wall to capture the wall effect while also saving computing time. A far field with an open boundary of 5000cm by 2400cm was developed around the mangrove tree to produce a computational model of the geometry and to minimize the boundary effect on the airflow. Grid-independent research was carried out using various mesh sizes to determine the best grid resolution for the analysis, which is shown in Figure 5.

The simulation of this study is performed using a mesh of 64,906,691 cells based on the Grid convergence study. Mesh of high quality was created with skewness less than 0.9 and the mesh is imported to Ansys fluent for CFD study.

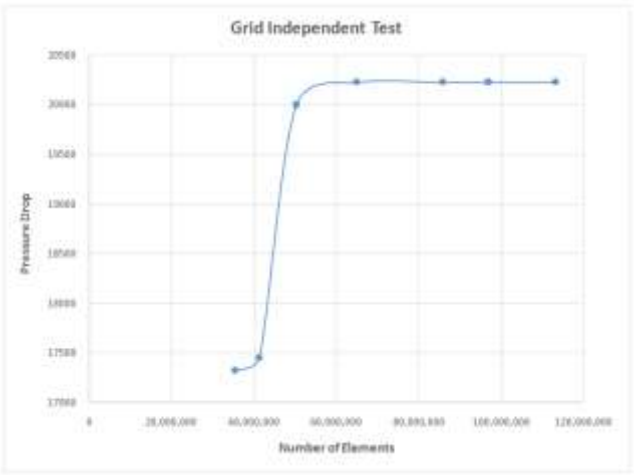

Fig. 5: Grid Independent study

2.5 Finite Volume Method

In this study, the Finite Volume Method is used. The first and foremost step in the finite volume method is to divide the entire domain under consideration into discrete cells or control volumes. Nodes are placed at the cell center and a grid is generated. Integration of the non-linear governing partial differential equation over each control volume is the key process of the finite volume method. This yields a system of discretized equations at the nodal points. The system is then solved to obtain the unknown values of velocity and pressure at the nodal points followed by post-processing of the results.

The integral forms of the non-linear partial differential equations are discretized over each control volume and transformed into an algebraic system of equations using the upwind difference scheme in the following manner.

Continuity equation:

$$\frac{(\rho uA)_{I,J} - (\rho uA)_{I-1,J}}{\Delta x} + \frac{(\rho vA)_{I,J} - (\rho vA)_{I,J-1}}{\Delta y} = 0 \quad (6)$$

X-momentum:

$$\frac{\left(\rho u_{I,J}^2 A\right) - (\rho u_{I-1,J}^2 A)}{\Delta x} + \frac{\left(\rho u_{i,j+1} A\right) v_{i,j+1} - (\rho u_{i,J} A)\, v_{i,j}}{\Delta y} = \frac{\left(p_{I-1,J} - p_{I,J}\right)}{\Delta x} \Delta U +$$

$$\left\{ \begin{matrix} \left[\frac{\left(\mu \frac{\partial u}{\partial x}\right)_{i+1,J} - \left(\mu \frac{\partial u}{\partial x}\right)_{i,J}}{\Delta x} \right] + \\ \left[\frac{\left(\mu \frac{\partial u}{\partial y}\right)_{i,j+1} - \left(\mu \frac{\partial u}{\partial y}\right)_{i,J}}{\Delta y} \right] \end{matrix} \right\} \Delta U \quad (7)$$

$$\left\{ \begin{matrix} \left[\frac{\left(\mu \frac{u_{i+1,J} - u_{i,J}}{\Delta x_{PE}}\right) - \left(\mu \frac{u_{i,J} - u_{i-1,J}}{\Delta x_{WP}}\right)}{\Delta x} \right] + \\ \left[\frac{\left(\mu \frac{u_{i,J+1} - u_{i,J}}{\Delta y_{NP}}\right)_{i,J+1} - \left(\mu \frac{u_{i,J} - u_{i,J-1}}{\Delta y_{PS}}\right)}{\Delta y} \right] \end{matrix} \right\} \Delta U \quad (8)$$

ΔU is the u-control volume.
Δx is the width of the u-control volume.

Y-momentum:

$$\frac{(\rho v_{I,J} A) u_{I,J} - (\rho v_{I-1,J} A) u_{I-1,J}}{\Delta x} + \frac{\left(\rho v_{i,j+1}^2 A\right) - (\rho v_{i,J}^2 A)}{\Delta y} = \frac{\left(p_{i,j} - p_{i,j+1}\right)}{\Delta y} \Delta V +$$

$$\left\{ \begin{matrix} \left[\frac{\left(\mu \frac{v_{i+1,J} - v_{i,J}}{\Delta x_{PE}}\right)_e - \left(\mu \frac{v_{i,J} - v_{i-1,J}}{\Delta x_{PW}}\right)_w}{\Delta x} \right] \\ \left[\frac{\left(\mu \frac{v_{i,J+1} - v_{i,J}}{\Delta y_{PW}}\right)_n - \left(\mu \frac{v_{i,J} - v_{i,J-1}}{\Delta y_{SP}}\right)_s}{\Delta y} \right] \end{matrix} \right\} \Delta V \quad (9)$$

ΔV is the v-control volume.
Δy is the width of the v-control volume.

Similarly, Z - momentum equation also can be calculated. The k-ε model is used to represent the impacts of turbulence in turbulent flow. In addition to the equations of continuity and momentum, the k-ε model provides two transport equations (10) to (11) for turbulent kinetic energy k and turbulent dissipation rate ε., are given by

$$\frac{\partial}{\partial t}(\rho k) + \frac{\partial}{\partial x_i}(\rho k u_i) = \frac{\partial}{\partial x_j}\left[\left(\mu + \frac{\mu_t}{\sigma_k}\right)\frac{\partial k}{\partial x_j}\right] + M_k + M_b - \rho\varepsilon - Y_m) \quad (10)$$

$$\frac{\partial}{\partial t}(\rho \varepsilon) + \frac{\partial}{\partial x_i}(\rho \varepsilon u_i) = \frac{\partial}{\partial x_j}\left[\left(\mu + \frac{\mu_t}{\sigma_\varepsilon}\right)\frac{\partial \varepsilon}{\partial x_j}\right] + C_{\varepsilon 1}\frac{\varepsilon}{k}(M_k + C_{\varepsilon 3}M_b) - C_{\varepsilon 2}\rho\frac{\varepsilon^2}{k} \quad (11)$$

where ui is the x-direction velocity component, μ is the viscosity, t is the turbulent viscosity, M_k is the kinetic energy production due to shear stress, M_b is the kinetic energy generation due to buoyancy, and Y_m is the kinetic energy production due to compressibility. The empirical constants are: $C_{\varepsilon 1}$=*1.44;* $C_{\varepsilon 2}$=*1.92;* $C_{\varepsilon 3}$=1.0; σ_k=1, σ_ε=1.3, and C_μ=0.09 are empirical constants.

For three-dimensional flows, it is given by,

$$a_{i,J,K}u_{i,J,K} = \sum a_{mbn}\, u_{mbn} + \frac{(p_{I+1,J,K} - p_{I-1,J,K})}{2\Delta x}\Delta V_u \quad (12)$$

$$a_{I,j,K}v_{I,j,K} = \sum a_{mbn}\, v_{mbn} + \frac{(p_{I,J+1,K} - p_{I,J-1,K})}{2\Delta y}\Delta V_v \quad (13)$$

$$a_{I,J,k}v_{I,J,k} = \sum a_{mbn}\, w_{mbn} + \frac{(p_{I,J,K+1} - p_{I,J,K-1})}{2\Delta y}\Delta V_w \quad (14)$$

The above equations (12) to (14) represent discretized Navier Stokes Equations for steady state flow where $\Delta V_u, \Delta V_v$ and ΔV_w are the volume of u-cell, v-cell and w-cell. For unsteady flow ap_0 in (15) is added to the central coefficients of the above three equations.

$$ap_0 = \rho\, p_0 \frac{\Delta v}{\Delta t} \quad (15)$$

2.6 Error Analysis

There are two kinds of errors made by the computer during each iteration. Which are the discretization error (D_E) and round off error(R)

$$De = A - S; \quad R = N - S \quad (16)$$

Where 'A' is the analytical solution of the partial differential equation. 'S' is the exact solution of the difference equation. 'N' is the Numerical solution from a real computer with finite accuracy. Discretization involves approximating continuous mathematical models with discrete counterparts. The error arises due to the finite representation of continuous quantities in the discrete domain. Round-off errors occur due to limitations in computer precision. Computers represent numbers with a finite number of digits, leading to small errors in calculations, especially with repeated operations.

The solution is unstable if the R_i's grow bigger during the progression of the solution from n^{th} step to $(n+1)^{th}$ step. The stable solution is obtained if

$$\left|\frac{R_i^{n+1}}{R_i^n}\right| \leq 1 \quad (17)$$

Stability is crucial for the reliability of numerical solutions. If the Ri's (round-off errors) grow larger during iterations, it indicates instability in the solution. The stability criterion (Equation 17) ensures that the errors do not accumulate rapidly, preventing numerical instability.

In summary, discretization errors result from the process of approximating continuous problems with discrete methods, while round-off errors stem from the finite precision of computer arithmetic. Ensuring stability through the defined criterion helps maintain the reliability of numerical solutions in the iterative process.

3 Results and Discussion

The velocity profile of both steady and unsteady air flow is analyzed and interpreted the graph at different positions y=0.25m, z=0.25m, y=0.75m&z=0.75m are visualized in Figure 6, Figure 7, Figure 8 and Figure 9 respectively. Both steady and unsteady flow shows a similar pattern and velocity contours, which are visualized in these figures.

The maximum flow velocity is 86 m/s (red color contour) and the minimum velocity is 0 m/s (stagnation area) as shown in all these figures (Figure 6, Figure 7, Figure 8 and Figure 9). The individual roots are located in some position and jet flow occurs around these roots, which causes the flow velocity to increase in certain locations. The velocity of the flow decreased to 0m/s when the flow traveled around the Rhizophora Mangrove roots and tree. The light blue color region is represented by a velocity of 21.5 m/s, the dark green colorcolor region is represented by a velocity of 43.0 m/s, the light green color region represented by 51.3 m/s, and some places in the main trunk represented by 77.4 m/s.

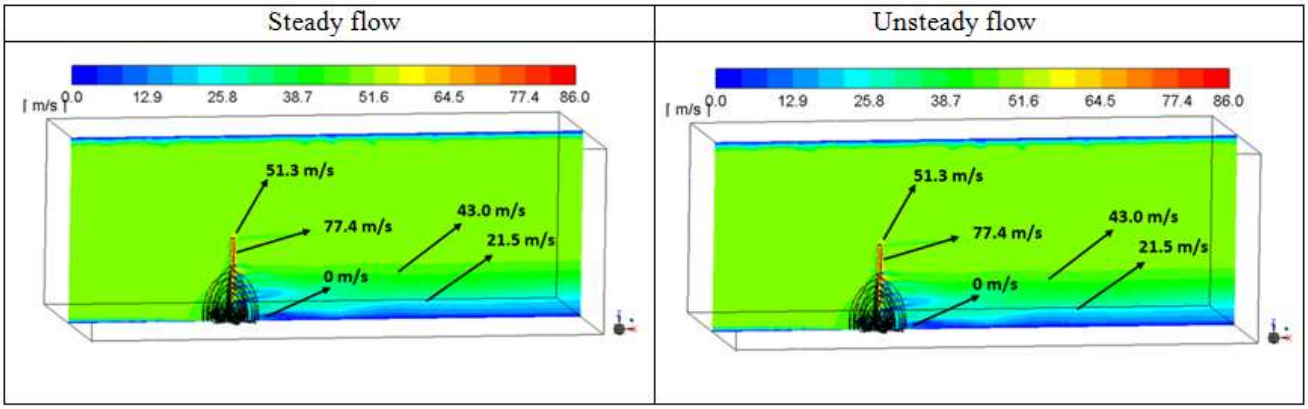

Fig. 6: Velocity at y=0.25m

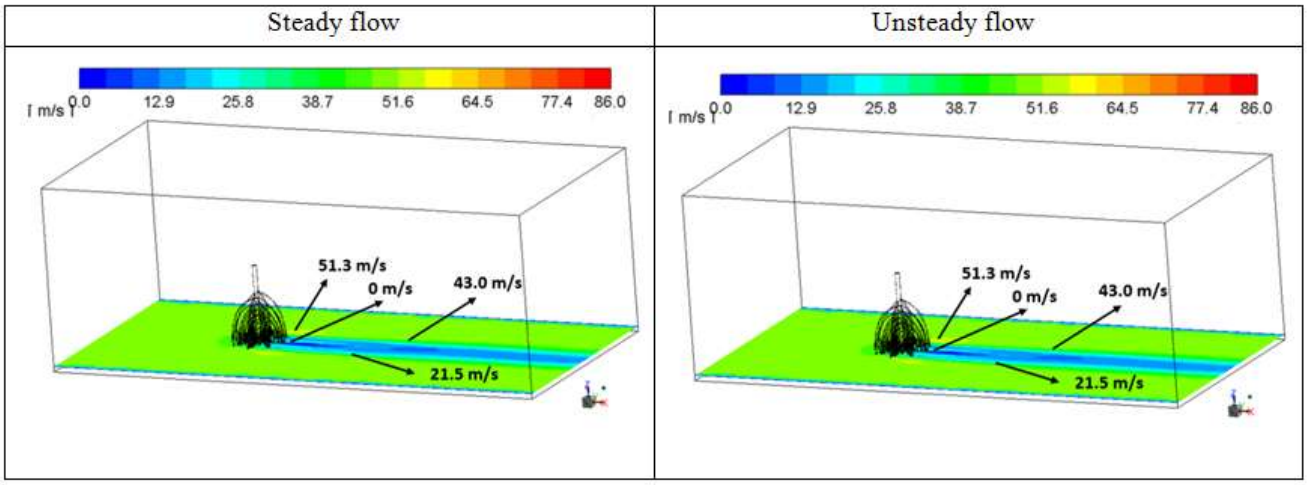

Fig. 7: Velocity at z=0.25m

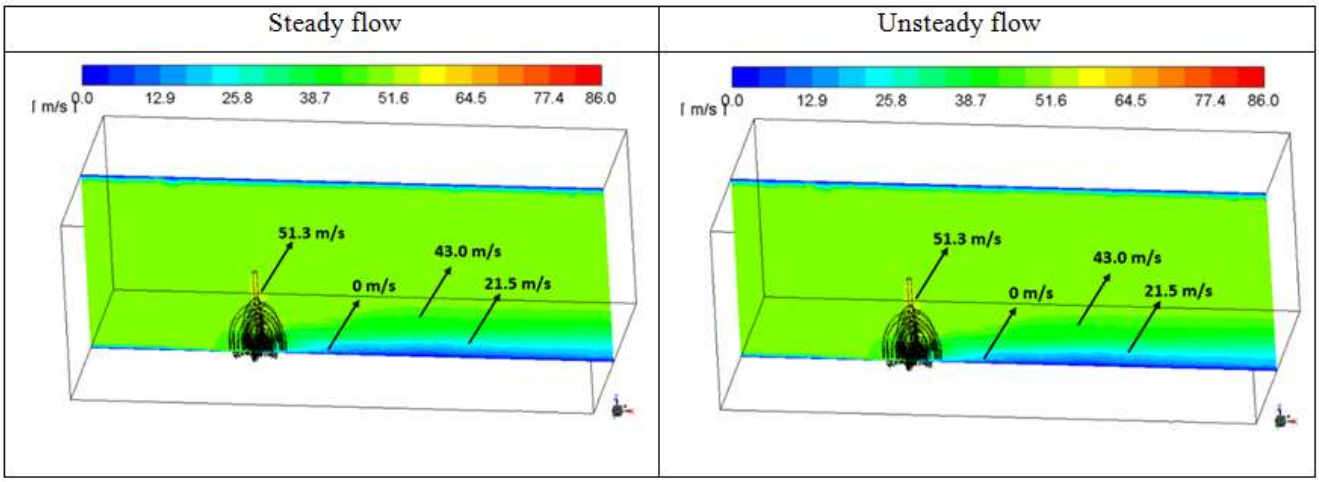

Fig. 8: Velocity at y=0.75

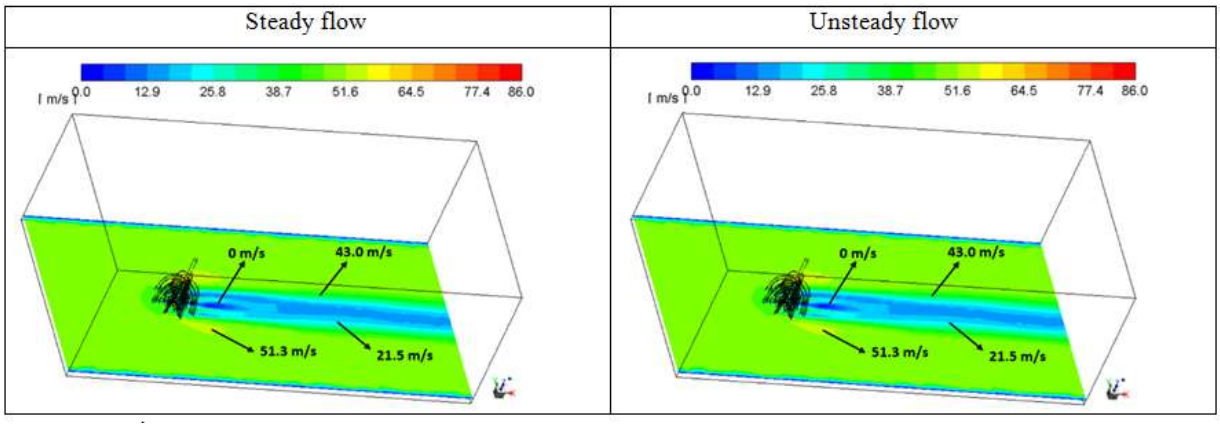

Fig. 9: Velocity at z=0.75m

The pressure distribution of both steady and unsteady wind flow is also analyzed and interpreted in the graph at different positions y=0.25m, z=0.25m, y=0.75m&z=0.75m are shown in Figure 10, Figure 11, Figure 12 and Figure 13 respectively. The highest pressure observed as 1679 Pa (red color contour).

The pressure decreased to -116 Pa (light blue color contour) after the flow passed through the mangroves. The green color contour is represented by the pressure of 140Pa and the yellow color contour indicates the pressure is 815 Pa.

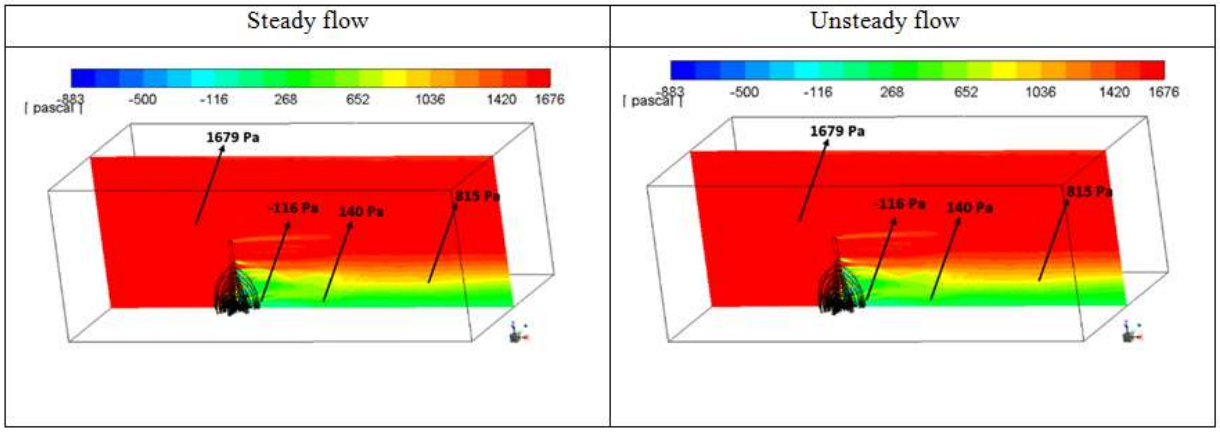

Fig. 10: Pressure at y=0.25m

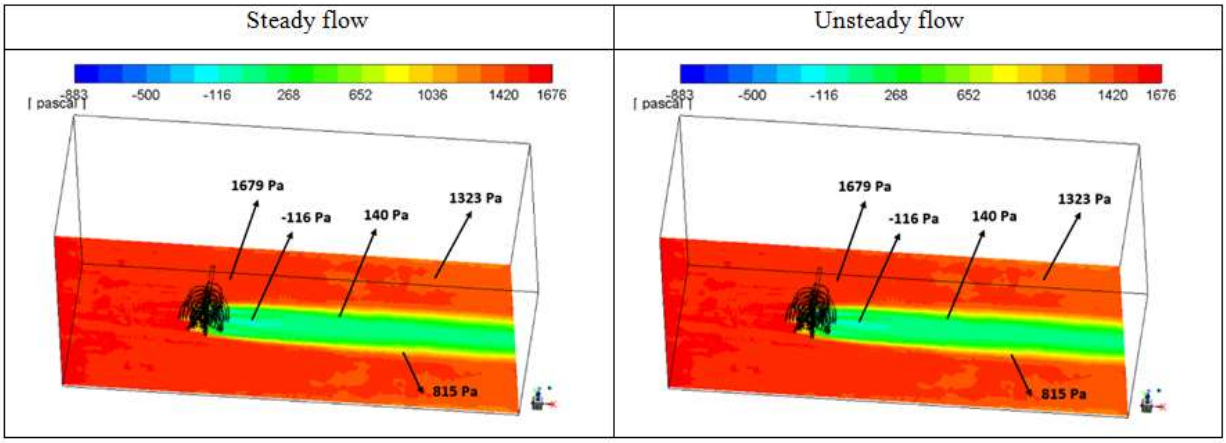

Fig. 11: Pressure at z=0.25m

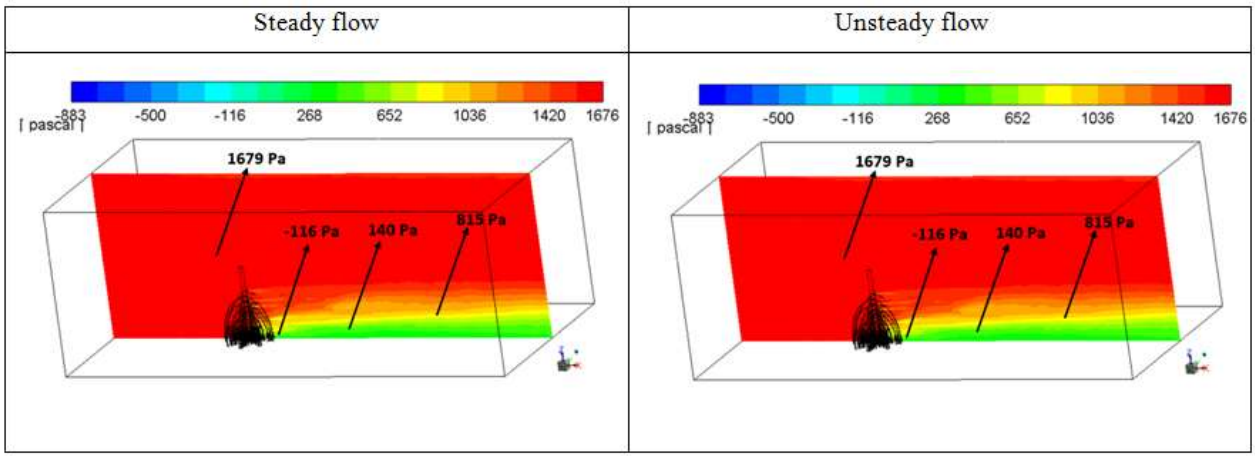

Fig. 12: Pressure at y=0.75m

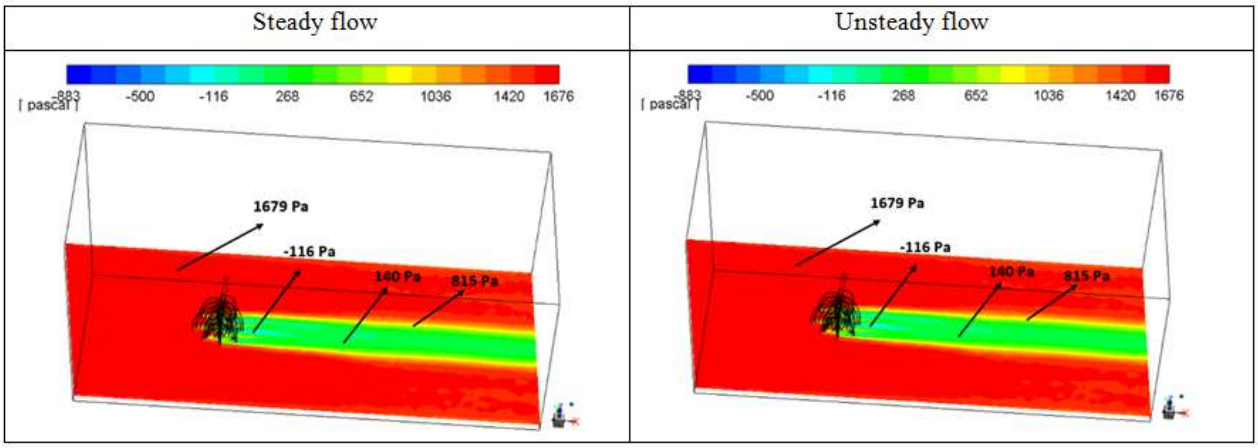

Fig. 13: Pressure at z=0.75m

Figure 14, demonstrates the drag coefficients and drag force on the model's wall tree. For air velocity of 50 m/s, the highest coefficient of drag is 20687.047 and the drag force is 12670.816. Figure 15, illustrates how the solution converges onto three decimal places when the fluid flow velocity is 50m/s in both steady and unsteady models. The convergence plot and a previous study from the literature survey, [25], [26], [27], [28], [31], [32], [34], are used to validate the outcome.

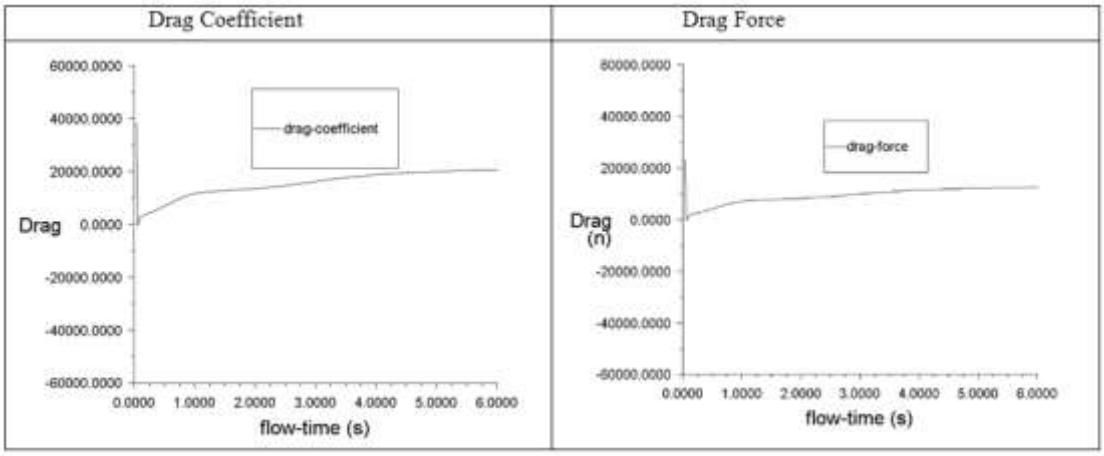

Fig. 14: Drag coefficient and drag force acting on wall tree

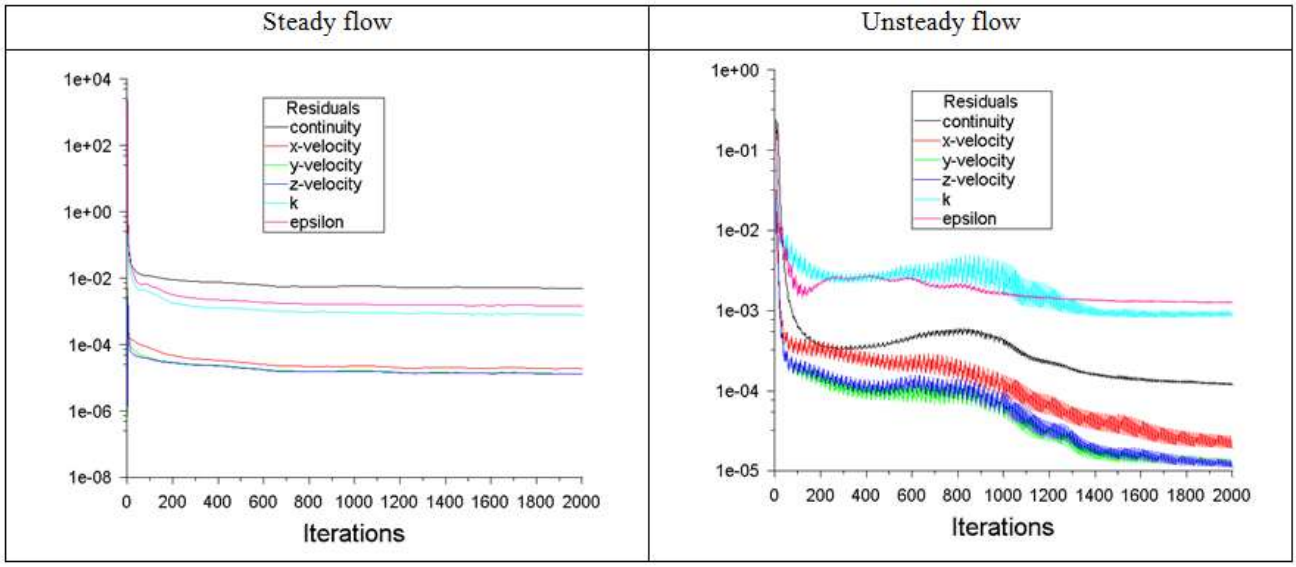

Fig. 15: Convergence plot

4 Conclusion

The CFD simulations of the steady and unsteady wind flow around a three dimensional Rhizophora mangrove tree model (using the data from the Pichavaram mangrove forest) with flow velocity of 50m/s were simulated and analyzed the velocity profile, pressure distribution, drag coefficient, and drag force. The ANSYS-18.1 Fluent with the k-epsilon, steady, and unsteady turbulent models are used for the simulations. This study reveals that the Rhizophora mangroves can decrease the velocity of the wind and be able to protect the coast. The Rhizophora mangrove trees in the Pichavaram can significantly reduce the flow velocity of the wind and will be able to safeguard the coast and communities nearby from natural disasters such as cyclones, mudslides, and tsunamis. The future scope of this research refers to the wave simulation around multiple mangrove trees, multiphase flow, and different arrangements of mangrove trees. This study advises each human to plant new mangrove trees and protect old ones because they are extremely valuable.

References:

[1] Danielsen, Finn, Mikael K. Sørensen, Mette F. Olwig, Vaithilingam Selvam, Faizal Parish, Neil D. Burgess, Tetsuya Hiraishi, Vagarappa M. Karunagaran, Michael S. Rasmussen, and Nyoman Suryadiputra. The Asian tsunami: a protective role for coastal vegetation. *Science* 310, no. 5748 (2005): 643-643.

[2] Lee, Shing Yip, Jurgene H. Primavera, Farid Dahdouh- Guebas, Karen McKee, Jared O. Bosire, Stefano Cannicci, Karen Diele, Francois Fromard, Nico Koedam, Cyril Marchand, Irving Mendelssohn, Nibedita Mukherjee, and Sydne Record. Ecological role and services of tropical mangrove ecosystems: a reassessment. *Global ecology and biogeography* 23, no. 7 (2014): 726-743.

[3] Rahuman, Sini, A. Mohamed Ismail, Shyla Manavalan Varghese, and George Kwamina Toworfe. Comparative Study of Flow Patterns around Rhizophora and Avicennia Mangrove Roots Using Computational Fluid Dynamics Simulation. *Advances in Materials Science and Engineering* 2022 (2022).

[4] Tanaka, Norio, Yasushi Sasaki, M. I. M. Mowjood, K. B. S. N. Jinadasa, and Samang Homchuen. Coastal vegetation structures and their functions in tsunami protection: experience of the recent Indian Ocean tsunami. *Landscape and ecological engineering* 3 (2007): 33-45.

[5] Medeiros, Stephen C. "Hydraulic Bottom Friction and Aerodynamic Roughness Coefficients for Mangroves in Southwest Florida, USA." *Journal of Marine Science and Engineering* 11, no. 11 (2023): 2053.

[6] Mazda, Yoshihiro, Eric Wolanski, Brian King, Akira Sase, Daisuke Ohtsuka, and Michimasa Magi. Drag force due to vegetation in mangrove swamps. *Mangroves and salt marshes* 1 (1997): 193-199.

[7] Massel, S. R., K. Furukawa, and R. M. Brinkman. Surface wave propagation in

mangrove forests. *Fluid Dynamics Research* 24, no. 4 (1999): 219.

[8] Hadi, Safwan, Hamzah Latief, and Muliddin Muliddin. Analysis of surface wave attenuation in mangrove forests. *Journal of Engineering and Technological Sciences* 35, no. 2 (2003): 89-108.

[9] Brinkman, Richard Michael. *Wave attenuation in mangrove forests: an investigation through field and theoretical studies*. PhD diss., James Cook University, 2006.

[10] Vo-Luong, Phuoc, and Stanislaw Massel. Energy dissipation in non-uniform mangrove forests of arbitrary depth. *Journal of Marine Systems* 74, no. 1-2 (2008): 603-622.

[11] Mei, Chiang C., I-Chi Chan, Philip L-F. Liu, Zhenhua Huang, and Wenbin Zhang. Long waves through emergent coastal vegetation. *Journal of Fluid Mechanics* 687 (2011): 461-491.

[12] Behera, H., S. Das, and T. Sahoo. Wave propagation through mangrove forests in the presence of a viscoelastic bed. *Wave motion* 78 (2018): 162-175.

[13] Das, Arijit, Soumen De, and B. N. Mandal. Small amplitude water wave propagation through mangrove forests having thin viscoelastic mud layer. *Waves in random and complex media* 32, no. 3 (2022): 1251-1268.

[14] Huang, Zhenhua, Yu Yao, Shawn Y. Sim, and Yao Yao. Interaction of solitary waves with emergent, rigid vegetation. *Ocean Engineering* 38, no. 10 (2011): 1080-1088.

[15] Ma, Gangfeng, James T. Kirby, Shih-Feng Su, Jens Figlus, and Fengyan Shi. Numerical study of turbulence and wave damping induced by vegetation canopies. *Coastal Engineering* 80 (2013): 68-78.

[16] Tang, Jun, Derek Causon, Clive Mingham, and Ling Qian. Numerical study of vegetation damping effects on solitary wave run-up using the nonlinear shallow water equations. *Coastal Engineering* 75 (2013): 21-28.

[17] Quevedo. J.M.D, Uchiyama. Y and Kohsaka. R (2020), "Perceptions of local communities on mangrove forests, their services and management: Implications for Eco-DRR and blue carbon management for Eastern Samar, Philippines", *Journal of Forest Research*, Vol. 25, No. 1, pp. 1-11.

[18] Maza. M, Lara. J. L and Losada. I. J (2019), "Experimental analysis of wave attenuation and drag forces in a realistic fringe Rhizophora mangrove forest", *Advances in Water Resources*, Vol. 131, p. 103376.

[19] Liu, Philip L-F., Che-Wei Chang, Chiang C. Mei, Pedro Lomonaco, Francisco L. Martin, and Maria Maza. Periodic water waves through an aquatic forest. *Coastal Engineering* 96 (2015): 100-117.

[20] Tang, Jun, Shaodong Shen, and Hui Wang. Numerical model for coastal wave propagation through mild slope zone in the presence of rigid vegetation. *Coastal Engineering* 97 (2015): 53-59.

[21] Maza, Maria, Javier L. Lara, and Inigo J. Losada. Tsunami wave interaction with mangrove forests: A 3-D numerical approach. Coastal Engineering 98 (2015): 33-54.

[22] Tang, Jun, Yongming Shen, Derek M. Causon, Ling Qian, and Clive G. Mingham. Numerical study of periodic long wave run-up on a rigid vegetation sloping beach. *Coastal Engineering* 121 (2017): 158-166.

[23] Park, Jong Ryul, Ho Seong Jeon, Yeon Myeong Jeong, and Dong Soo Hur. Numerical analysis on energy dissipation of tsunami through vegetation zone. *Journal of Coastal Research* 79 (2017): 194-198.

[24] Burger, B. *Wave attenuation in mangrove forests*. (2005), TU Delft Repository.

[25] Abdul Aziz, Nuraini, Othman Inayatullah, and Mohamad Zamin Bin Mohamad Jusoh. The mechanism of mangrove tree in wave energy propagation. *Advanced Materials Research* 614 (2013): 568-572.

[26] Jusoh, Mohamed Zamin Mohamad, Nuraini Abdul Aziz, and Othman Inayatullah. Computational fluid dynamics simulation of flow velocities dissipation by mangrove roots. *ARPN journal of engineering and applied sciences* (2016).

[27] Amma, P. K. G., & Bhaskaran, P. K. (2020). Role of mangroves in wind-wave climate modeling–A review. *Journal of Coastal Conservation*, *24*, 1-14.

[28] Chang, C. W., & Mori, N. (2021). Green infrastructure for the reduction of coastal disasters: A review of the protective role of coastal forests against tsunami, storm surge, and wind waves. *Coastal Engineering Journal*, *63*(3), 370-385.

[29] Das, S., & Crépin, A. S. (2013). Mangroves can provide protection against wind damage during storms. *Estuarine, Coastal and Shelf Science*, *134*, 98-107.

[30] Teh, Su Yean, Hock Lye Koh, Philip Li–Fan Liu, Ahmad Izani Md Ismail, and Hooi Ling Lee. Analytical and numerical simulation of tsunami mitigation by mangroves in Penang, Malaysia. *Journal of Asian Earth Sciences* 36, no. 1 (2009): 38-46.

[31] Zhang, X., H. Cheong, and V. Chua. An investigation on the geometrical properties of the root system of mangrove and its influence on flow. *In Proceedings of the 18th Congress of the Asia and Pacific Division of the International Association for Hydro-Environment Engineering and Research*. 2012.

[32] Vo-Luong, Phuoc, and Stanislaw Massel. Energy dissipation in non-uniform mangrove forests of arbitrary depth. *Journal of Marine Systems* 74, no. 1-2 (2008): 603-622.

[33] Vinayakumar, B., Antony Rahul, V. A. Binson, and Sunny Youhan. Gravitational water vortex: Finite element analysis based design and implementation. *Chemical and Process Engineering* 43, no. 3 (2022).

[34] Rahuman, Sini, A. Mohamed Ismail, Shyla Manavalan Varghese, George Kwamina Toworfe, and Bashyam Sasikumar. Wind Flow Simulation around Rhizophora Mangrove Roots Using Computational Fluid Dynamics. *Journal of Nanomaterials*, 2022 (2022).

Contribution of Individual Authors to the Creation of a Scientific Article (Ghostwriting Policy)

The authors equally contributed to the present research, at all stages from the formulation of the problem to the final findings and solution.

Sources of Funding for Research Presented in a Scientific Article or Scientific Article Itself

No funding was received for conducting this study.

Conflict of Interest

The authors have no conflicts of interest to declare.